Supporting Information

Lithium Stabilizes Square Two-Dimensional Metal Sheets: A Computational Exploration

Jie Li[a,#], Yu Liu[a,#], Linke Yu[a], Haihong Meng[a], Jinxing Gu[b], Fengyu Li[a,*]

[a] *School of Physical Science and Technology, Inner Mongolia University, Hohhot, 010021, P.R.China*

[b] *Department of Chemistry, The Institute for Functional Nanomaterials, University of Puerto Rico, Rio Piedras Campus, San Juan, PR 00931, USA*

*Corresponding Author: fengyuli@imu.edu.cn (FL)

[#] Equal contribution to this work

Table S1. The reaction pathway and the $\Delta ZPE - T\Delta S$ (in eV) of forming the intermediates on the M_2Li-I sheets.

	$*CO_2$	*COOH/*OCHO	*HCOOH	*HCO
Sb_2Li-I	0.46	0.19/0.23	/	/
Bi_2Li-I	0.46	0.24/0.27	/	/
Ag_2Li-I	0.46	0.21/0.22	0.30	-0.47
Au_2Li-I	0.46	0.22/0.23	/	/

Table S2. Space group (SG), cohesive energy, lattice parameters and bond lengths of the 2D M_2Li sheets. The E_{coh} in parenthesis refer to the square M monolayer. The length data in parenthesis denote the bond length in the M_4Li_2 clusters of D_{4h} symmetry.

	SG	**Symmetry**	E_{coh} **(eV/atom)**	***a* (Å)**	***b* (Å)**	**M−M (Å)**	**M−Li (Å)**
Al_2Li-I	*P*4/*mmm*	D^1_{4h}	-2.59 (-1.75)	2.69	2.69	2.69 (2.64)	2.92 (2.84)
Ga_2Li-I	*P*4/*mmm*	D^1_{4h}	-2.28 (-1.61)	2.66	2.66	2.66 (2.60)	2.93 (2.79)
In_2Li-I	*P*4/*mmm*	D^1_{4h}	-2.04 (-1.40)	3.12	3.12	3.12 (3.05)	3.00 (3.00)
Tl_2Li-I	*P*4/*mmm*	D^1_{4h}	-1.80 (-1.26)	3.32	3.32	3.32 (3.18)	3.10 (3.06)
Ge_2Li-I	*P*4/*mmm*	D^1_{4h}	-3.40 (-2.83)	2.74	2.74	2.74 (2.57)	2.80 (2.79)
Sn_2Li-I	*P*4/*mmm*	D^1_{4h}	-2.91 (-1.92)	3.09	3.09	3.09 (2.92)	3.03 (2.91)
Pb_2Li-I	*P*4/*mmm*	D^1_{4h}	-2.85 (-2.38)	3.24	3.24	3.24 (3.35)	3.11 (3.06)
Sb_2Li-I	*P*4/*mmm*	D^1_{4h}	-2.46 (-3.40)	3.12	3.12	3.12 (3.05)	3.00 (2.74)
Bi_2Li-I	*P4/mmm*	D^1_{4h}	-2.35 (-3.35)	3.26	3.26	3.26 (3.10)	3.11 (2.82)
Cu_2Li-I	*P*4/*mmm*	D^1_{4h}	-2.52 (-1.77)	2.47	2.47	2.47 (2.44)	2.59 (2.44)
Ag_2Li-I	*P4/mmm*	D^1_{4h}	-2.25 (-1.32)	2.83	2.83	2.83 (2.84)	2.77 (2.57)
Au_2Li-I	*P4/mmm*	D^1_{4h}	-2.69 (-2.04)	2.77	2.77	2.78 (2.84)	2.73 (2.52)
Hg_2Li-I	*P*4/*mmm*	D^1_{4h}	-0.75 (-0.54)	3.10	3.10	3.10 (3.37)	2.92 (2.81)
Sb_2Li-II	*P*21/*m*	C^2_{2h}	-2.44	3.06	11.21	3.01/3.11	2.95/3.11
Sb_2Li-III	*Pmmm*	D^1_{2h}	-2.41	3.02	3.04	4.94	2.89
Sb_2Li-IV	*P*6*mm*	C^1_{6v}	-2.16	5.15	5.15	2.97	3.01
Sb_2Li-V	*P*6*mm*	C^1_{6v}	-2.14	6.21	6.21	3.11/3.34	2.82
Sb_2Li-VI	*P4/mmm*	D^1_{4h}	-1.73	4.88	4.88	3.45	2.44
Bi_2Li-II	*P*21/*m*	C^2_{2h}	-2.31	3.21	11.81	3.25/3.24	3.22/3.00
Bi_2Li-III	*Pmmm*	D^1_{2h}	-2.26	3.19	3.20	5.03	2.98
Bi_2Li-IV	*P*6*mm*	C^1_{6v}	-2.03	5.36	5.36	3.09	3.13
Bi_2Li-V	*P*6*mm*	C^1_{6v}	-2.05	6.50	6.50	3.25/3.49	2.91
B_2Li-VI	*P4/mmm*	D^1_{4h}	-1.67	5.07	5.07	3.59	2.54
Ag_2Li-II	*P*21/*m*	C^2_{2h}	-2.18	2.80	10.25	2.78/2.80	2.81/2.69
Ag_2Li-III	*Pmmm*	D^1_{2h}	-2.14	2.82	2.71	4.50	2.66
Ag_2Li-IV	*P*6*mm*	C^1_{6v}	-2.03	4.77	4.77	2.76	2.80
Ag_2Li-V	*P*6*mm*	C^1_{6v}	-2.10	5.50	5.50	2.95/2.75	3.35/2.64
Ag_2Li-VI	*P4/mmm*	D^1_{4h}	-1.30	4.82	4.82	3.41	2.41
Au_2Li-II	*P*21/*m*	C^2_{2h}	-2.60	2.77	10.19	2.73/2.78	2.61/2.78
Au_2Li-III	*Pmmm*	D^1_{2h}	-2.57	2.77	2.72	4.32	2.57
Au_2Li-IV	*P*6*mm*	C^1_{6v}	-2.50	4.68	4.68	2.70	2.74
Au_2Li-V	*P*6*mm*	C^1_{6v}	-2.48	5.43	5.43	2.72/2.98	2.58
Au_2Li-VI	*P4/mmm*	D^1_{4h}	-1.88	4.65	4.65	3.29	2.33

Table S3. Space group (SG), cohesive energy, lattice parameters and bond lengths of the square M (Al, Ga, In, Tl, Ge, Sn, Pb, Sb, Bi, Cu, Ag, Au, Hg) monolayers.

	SG	Symmetry	E_{coh} (eV/atom)	*a* (Å)	*b* (Å)	M−M (Å)
Al	*P*4/*mmm*	D^1_{4h}	-2.58	2.63	2.63	2.63
Ga	*P*4/*mmm*	D^1_{4h}	-2.23	2.59	2.59	2.59
In	*P*4/*mmm*	D^1_{4h}	-1.90	2.96	2.96	2.96
Tl	*P*4/*mmm*	D^1_{4h}	-1.64	3.10	3.10	3.10
Ge	*P*4/*mmm*	D^1_{4h}	-3.66	2.59	2.59	2.59
Sn	*P*4/*mmm*	D^1_{4h}	-2.57	2.99	2.99	2.99
Pb	*P*4/*mmm*	D^1_{4h}	-2.71	3.15	3.15	3.15
Sb	*P*4/*mmm*	D^1_{4h}	-2.10	2.97	2.97	2.97
Bi	*P4/mmm*	D^1_{4h}	-1.97	3.13	3.13	3.13
Cu	*P*4/*mmm*	D^1_{4h}	-2.45	2.38	2.38	2.38
Ag	*P4/mmm*	D^1_{4h}	-1.79	2.72	2.72	2.72
Au	*P4/mmm*	D^1_{4h}	-2.43	2.67	2.67	2.67
Hg	*P*4/*mmm*	D^1_{4h}	-0.07	2.83	3.66	3.66

Table S4. The E_{coh} (in eV per atom) of M_2Li-I sheets and bulk M_mLi_n, space group (SG) of bulk M_mLi_n. Data in parenthesis refer to the E_{coh} of M bulk.

system	E_{coh}	M_mLi_n bulk	SG	E_{coh}
Al_2Li-I	-2.59 (-3.52)	Al_2Li_3 [i]	*R3 m*	-2.55
Ga_2LI-I	-2.28 (-2.68)	Ga_2Li [ii]	*Cmcm*	-2.25
In_2Li-I	-2.04 (-2.42)	$InLi_2$ [ii]	*Cmcm*	-2.13
Tl_2Li-I	-1.80 (-4.08)	TlLi [iii]	*Pm3̄m*	-2.04
Ge_2Li-I	-3.40 (-5.21)	GeLi [iv]	*I4₁/a*	-2.93
Sn_2Li-I	-2.91 (-3.17)	SnLi [v]	*P2/m*	-3.99
Pb_2Li-I	-2.85 (-3.31)	PbLi [vi]	*Pm3̄m*	-2.71
Sb_2Li-I	-2.46 (-2.67)	$SbLi_2$ [vii]	*P-62c*	-2.54
Bi_2Li-I	-2.35 (-2.52)	BiLi [viii]	*P4/mmm*	-2.45
Cu_2Li-I	-2.52 (-3.48)	--	--	--
Ag_2Li-I	-2.2 (-2.49)	AgLi [ix]	*Fm3̄m*	-2.26
Au_2Li-I	-2.69 (-2.98)	$AuLi_3$ [x]	*Fm3̄m*	-2.34
Hg_2Li-I	-0.75 (-1.67)	Hg_3Li [xi]	*P6₃/mmc*	-0.72
Li bulk	-1.57			

[i] K.F. Tebbe, H.G. von Schnering, B. Rueter and G. Rabeneck, Zeitschrift fuer Naturforschung. Teil B. Anorganische Chemie, Organische Chemie, 1973, **28**, 600.

[ii] J. Stoehr, W. Mueller and H. Schaefer, Studies in Inorganic Chemistry, 1983, **3**, 753.

[iii] W. Baden, P.C. Schmidt and A. Weiss, Physica Status Solidi, A, 1979, **51**, 183.

[iv] E. Menges, V. Hopf, H. Schaefer and A. Weiss, Zeitschrift fuer Naturforschung, Teil B. Anorganische Chemie, Organische Chemie, 1969, **24**, 1351.

[v] W. Mueller and H. Schaefer, Zeitschrift fuer Naturforschung, Teil B. Anorganische Chemie, Organische Chemie, 1973, **28**, 246.

[vi] H.N. Nowotny, Zeitschrift fuer Metallkunde, 1941, **33**, 388.

[vii] W. Mueller, Darstellung und Struktur der Phase Li_2Sb Zeitschrift fuer Naturforschung, Teil B. Anorganische Chemie, Organische Chemie, 1977, **32**, 357-359.

[viii] E. Zintl and G. Brauer, Zeitchrift fur Elektrochemie, 1935, **41**, 297.

[ix] R. W. G. Wyckoff, Second edition. Interscience Publishers, New York, New York Note: CsCl structure, cesium chloride structure Crystal Structures, 1963, **1**, 85-237.

[x] J. Verma, and G. Kienast, Das Verhalten der Alkalimetalle zu Kupfer, Silber und Gold Zeitschrift fuer Anorganische und Allgemeine Chemie, 1961, **310**, 143-169.

[xi] E. Zintl and A. Schneider, Zeitschrift fuer Elektrochemie und Angewandte Physikalische Chemie, 1935, **41**, 771.

Table S5. The computed elastic constants (C_{11}, C_{22}, C_{12}, C_{44}, in N/m) of the M_2Li-I monolayers. The mechanically stable M_2Li-I was highlighted in bold.

	C_{11}	C_{22}	C_{12}	C_{44}
Al_2Li-I	34.83	34.83	-2.19	1.02
Ga_2Li-I	22.89	22.89	80.75	-5.97
In_2Li-I	-7.82	-7.82	9.68	15.28
Tl_2Li-I	28.36	28.36	16.05	8.61
Ge_2Li-I	80.83	80.83	15.18	34.41
Sn_2Li-I	83.69	83.69	-20.49	27.77
Pb_2Li-I	10.28	10.28	-51.91	10.43
Sb_2Li-I	71.55	71.55	-17.38	18.26
Bi_2Li-I	68.95	68.95	-21.77	3.66
Cu_2Li-I	110.49	110.49	14.33	-6.98
Ag_2Li-I	72.91	72.91	-2.04	5.96
Au_2Li-I	122.32	122.32	10.08	22.05
Hg_2Li-I	34.84	34.84	-2.19	1.02

Table S6. The lowest adsorption energies of H, CO_2 (E_{ad}, in eV)) and the free energy change (ΔG, in eV) for forming *COOH and *OCHO on the M_2Li-I (M = Sb, Bi, Ag and Au).

Metal	E_{ad}(H)	E_{ad}(CO_2)	$\Delta G_{(*COOH)}$	$\Delta G_{(*OCHO)}$
Sb_2Li-I	/	**-0.09**	2.26	1.87
Bi_2Li-I	/	**-0.15**	1.79	0.75
Ag_2Li-I	2.17	**-0.23**	1.46	**0.40**
Au_2Li-I	/	**-0.42**	1.74	0.97

Table S7. The adsorption energies of H (E_{ad}, in eV) on the Ag_2Li-I.

Site	E_{ad}
bridge	2.19
top	**2.17**
hollow	2.23

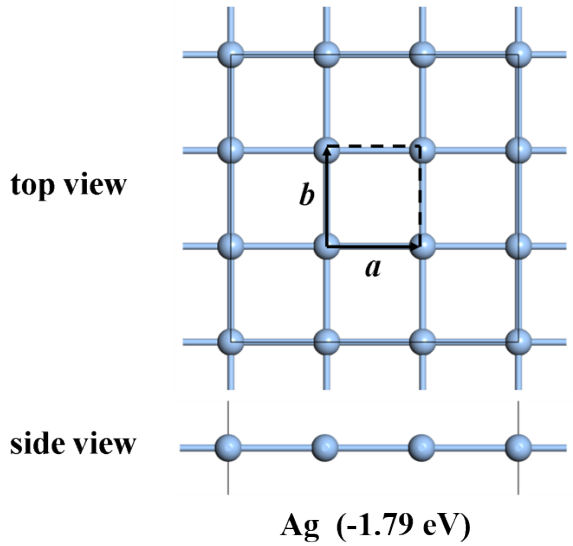

Fig. S1 Top and side views of the square M (represented by Ag structure) monolayer, *a* and *b* represent the lattice vectors. Data in parenthesis are the cohesive energies per atom.

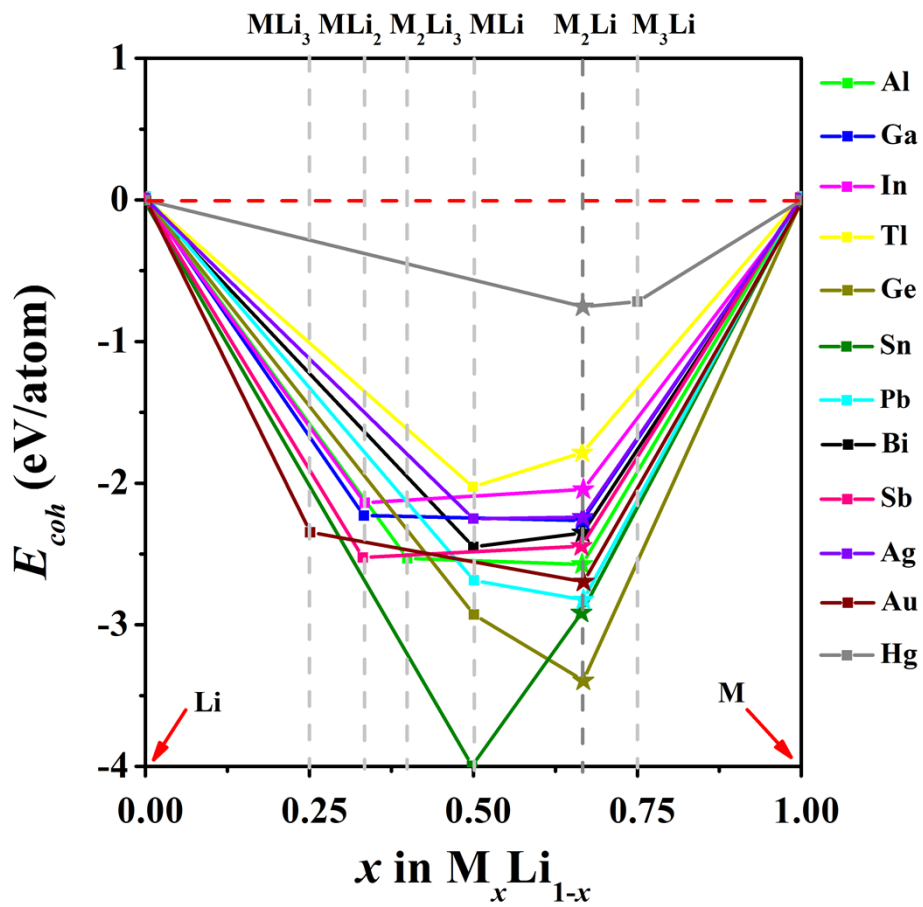

Fig. S2 The convex hull diagram of the M_xLi_{1-x} system, the "star" in the figure corresponding to our M_2Li-I (M = Al, Ga, In, Tl, Ge, Sn, Pb, Bi, Sb, Ag, Au and Hg) systems.

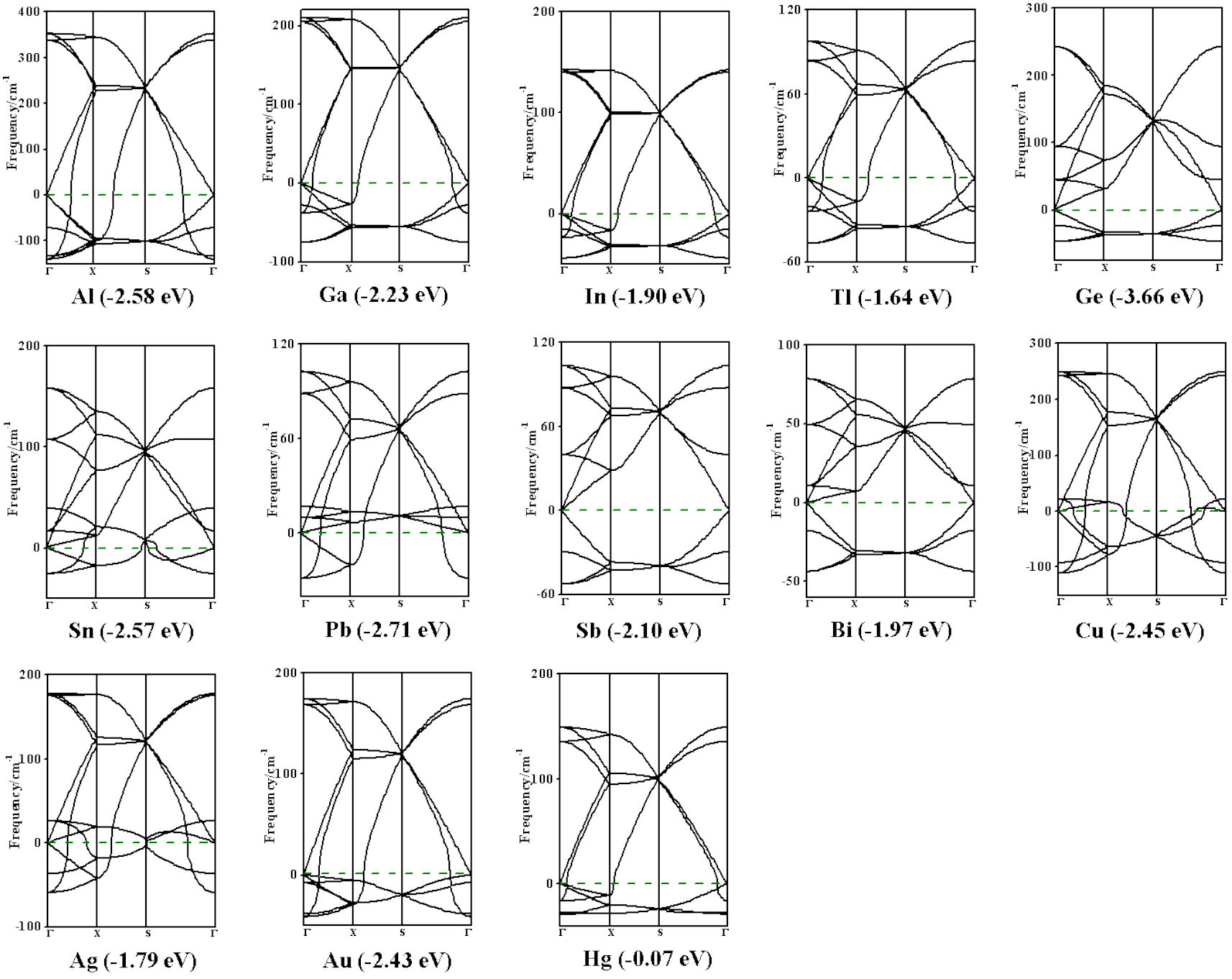

Fig. S3 The computed phonon dispersions of the square M monolayers. Data in parenthesis are the cohesive energies per atom.

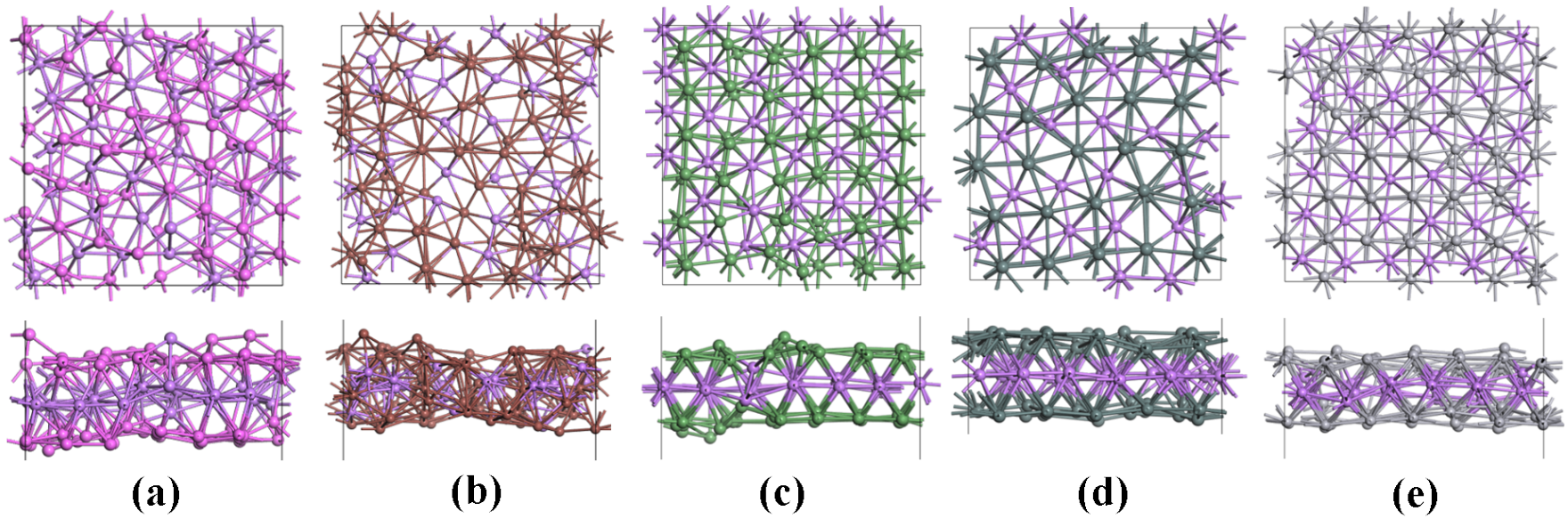

Fig. S4 The final structures of M_2Li-I monolayers through 5 ps's FPMD simulations at 300 K: Al_2Li-I (a), Tl_2Li-I (b), Ge_2Li-I (c), Sn_2Li-I (d), and Hg_2Li-I (e).

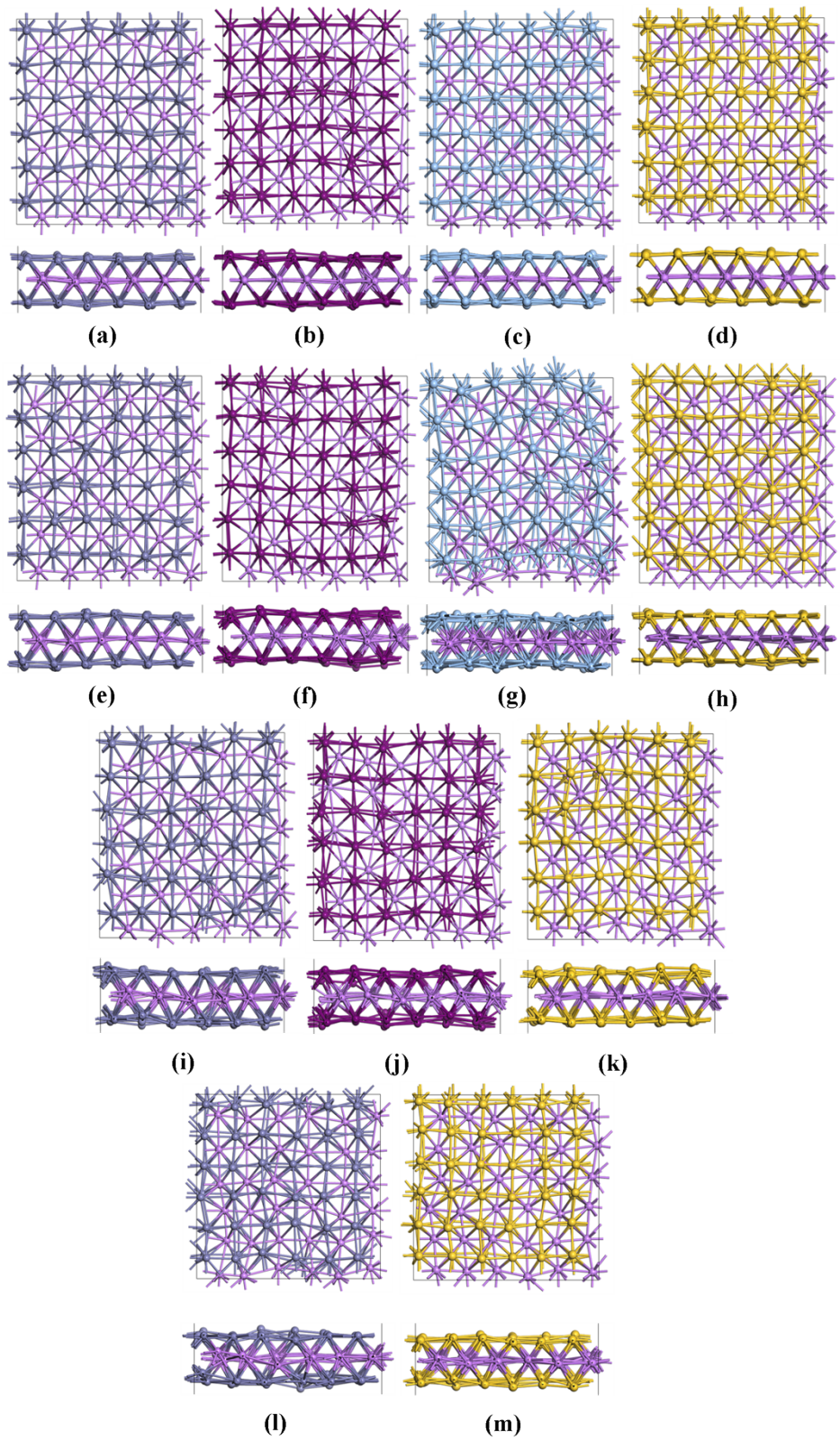

Fig. S5 Two views of the final structures of M_2Li-I monolayers through 5 ps's FPMD simulations: Sb_2Li-I (a), Bi_2Li-I (b), Ag_2Li-I (c) and Au_2Li-I (d) at 300 K; Sb_2Li-I (e), Bi_2Li-I (f), Ag_2Li-I (g) and Au_2Li-I (h) at 500 K; Sb_2Li-I (i), Bi_2Li-I (j) and Au_2Li-I (k) at 800 K; Sb_2Li-I (l) and Au_2Li-I (m) at 1000 K, respectively.

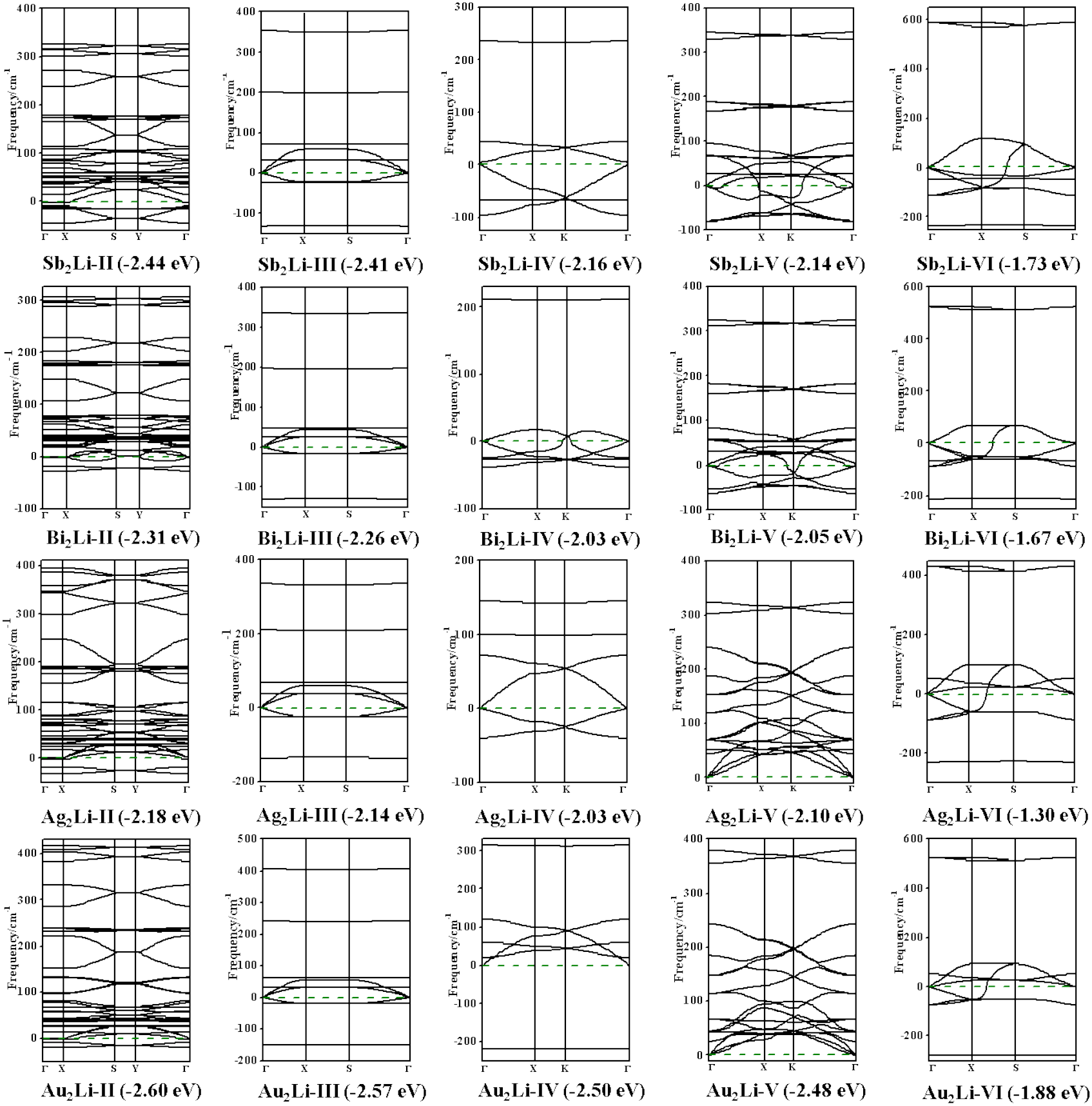

Fig. S6 The computed phonon dispersions of the PSO searched M_2Li sheets. Data in parenthesis are the cohesive energies per atom.

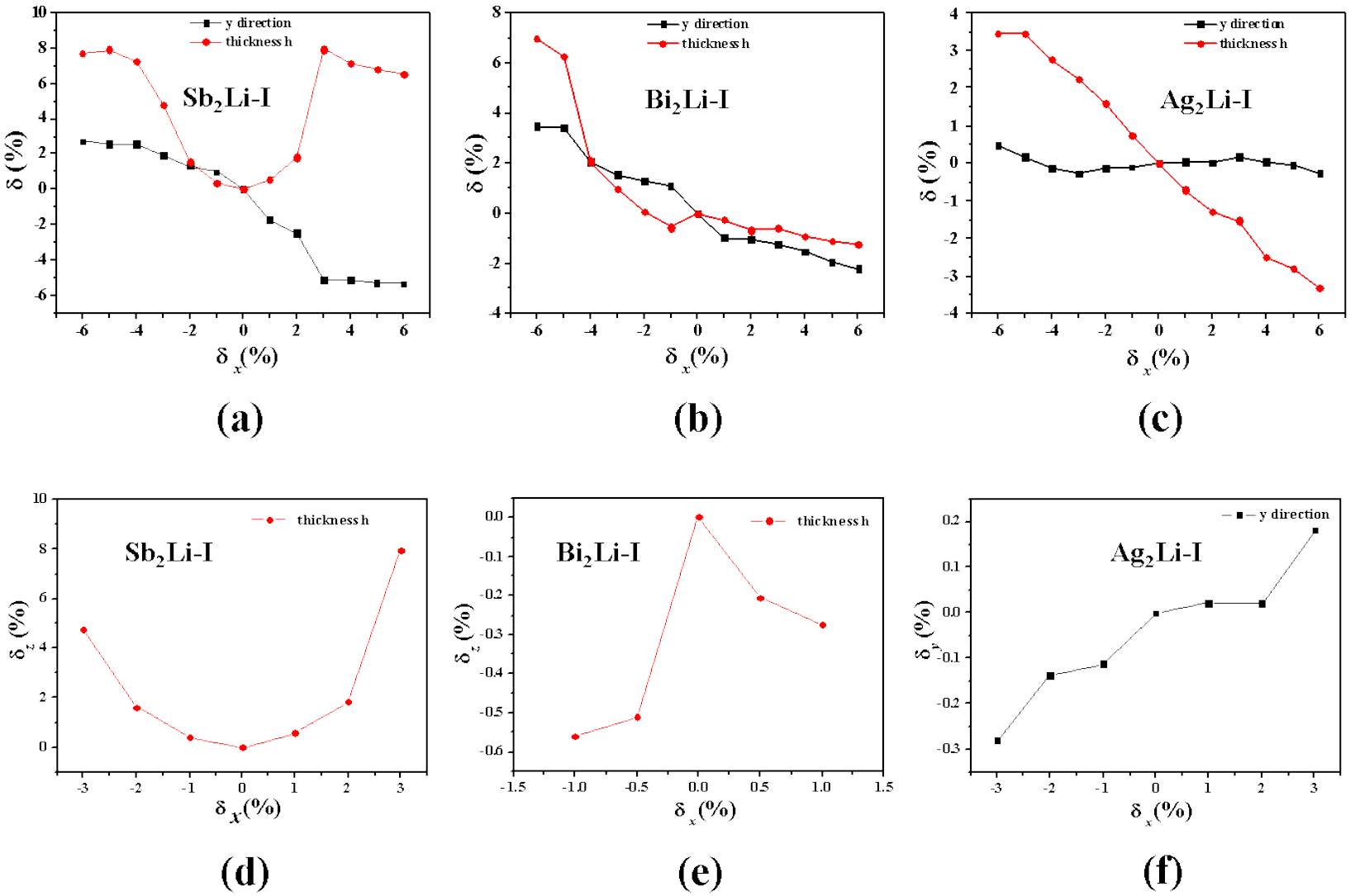

Fig. S7 Mechanical response (δ_y and thickness δ_z) of the Sb_2Li-I (a), Bi_2Li-I (b), and Ag_2Li-I (c) monolayers under the uniaxial strain along the *x* direction (δ_x ranging from -6% to 6%). Mechanical response (δ_y or thickness δ_z) of the half-auxetic Sb_2Li-I (d), Bi_2Li-I (e) and Ag_2Li-I (f) sheets under the uniaxial strain along the *x* direction (δ_x ranging from -3% to 3%).

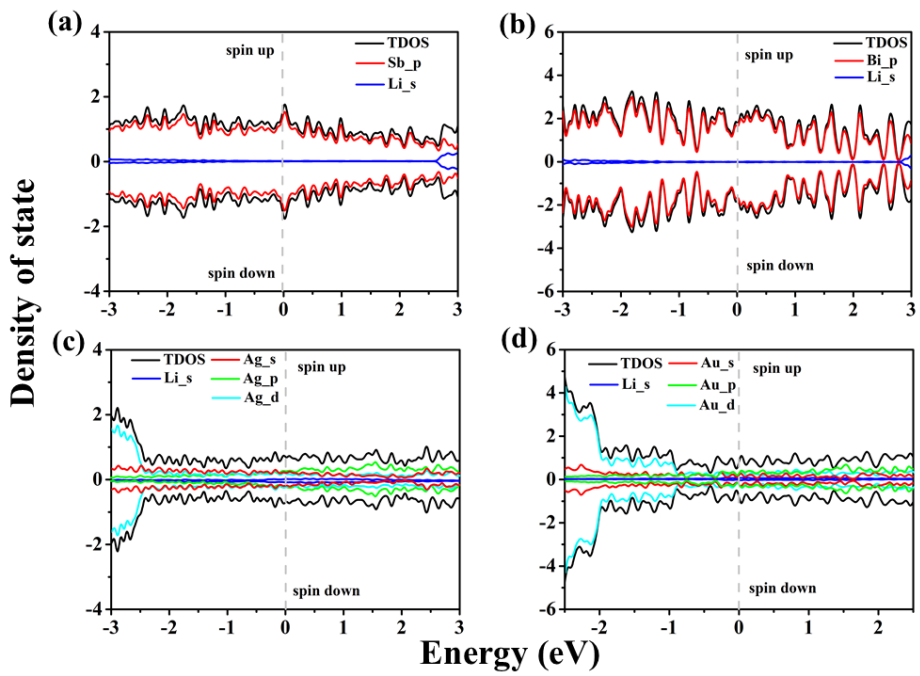

Fig. S8 Projected density of state (PDOS) considering spin polarization of M_2Li-I monolayers: (a) Sb_2Li-I, (b) Bi_2Li-I, (c) Ag_2Li-I and (d) Au_2Li-I. The Fermi level was assigned at 0 eV.

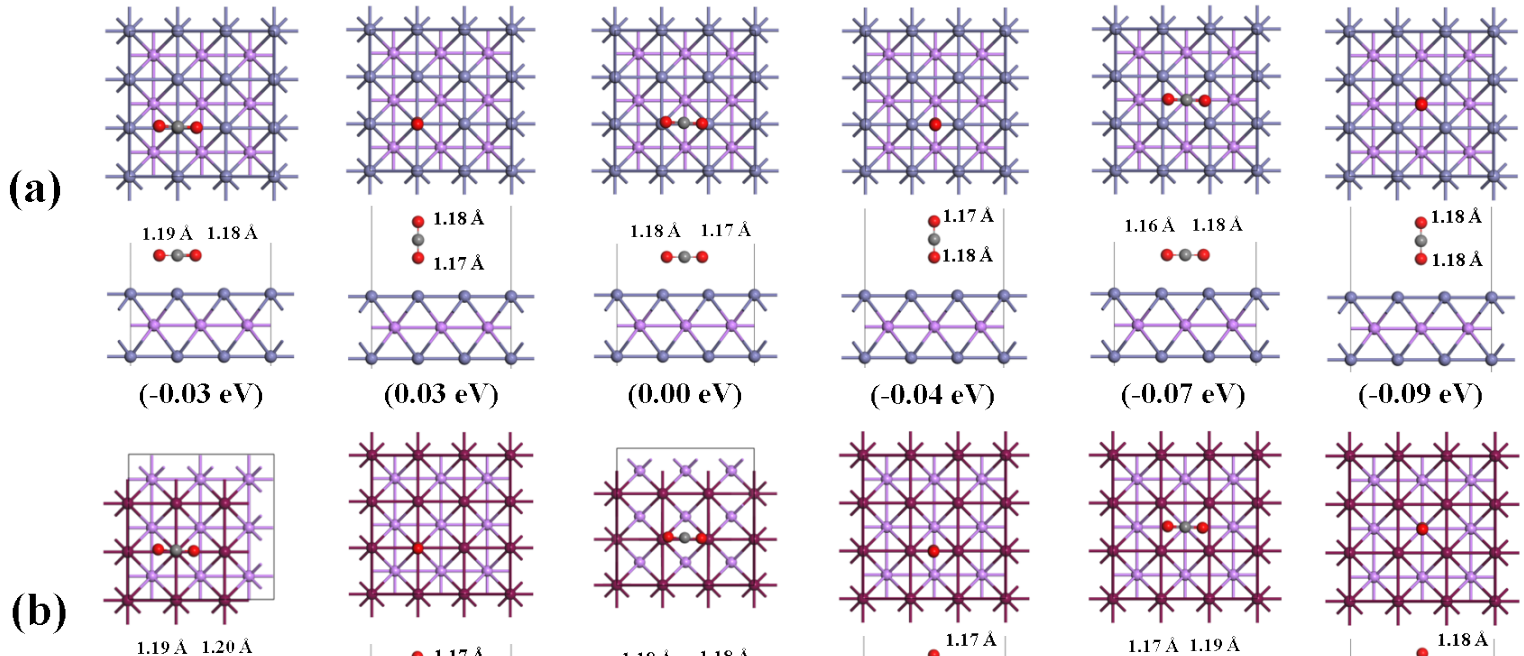

Fig. S9 Top and side views of the optimized structures of CO_2 adsorbed at different site of the Sb_2Li-I (a), Bi_2Li-I (b), Ag_2Li-I (c) and Au_2Li-I (d). The adsorption energy of CO_2 and the C−O bond lengths were given in the corresponding structure.

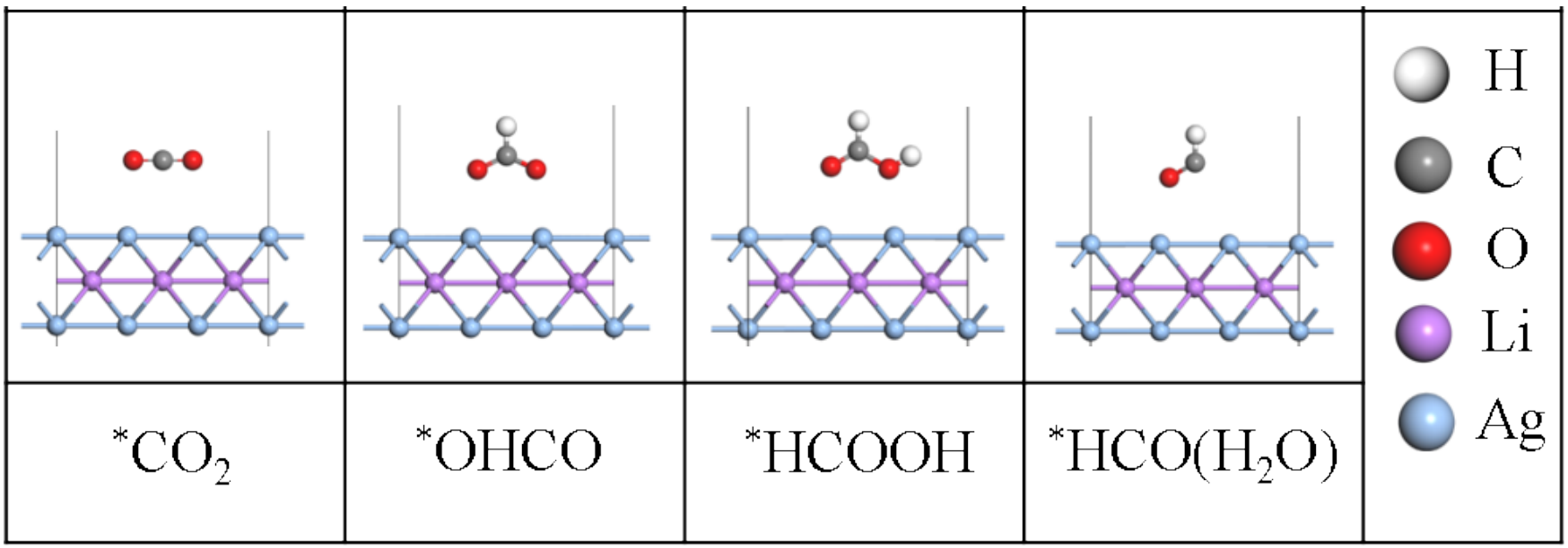

Fig. S10 The optimized structures of the intermediates along the optimal CO_2RR route on the Ag_2Li-I.

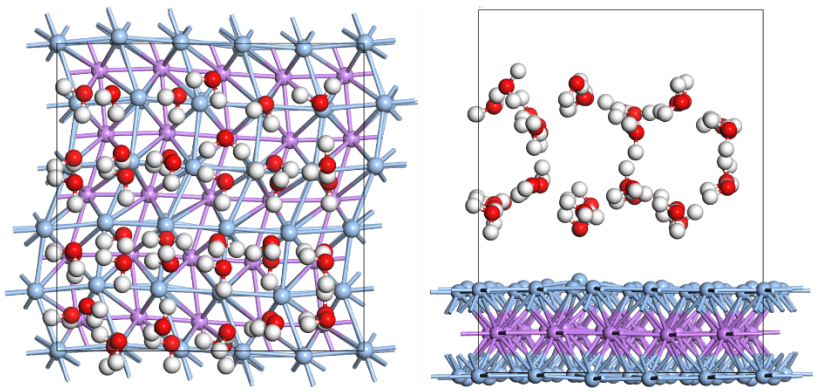

Fig. S11 The final structures of Ag_2Li-I with water through 5 ps's FPMD simulation at 300 K.